3×2 reconstruction of the Sm/Si(111) interface

Frank Palmino,* Eric Ehret, Louay Mansour, and Jean-Claude Labrune
CREST, CNRS UMR 6000, 4 place Tharradin, Boîte Postale 71427, 25211 Montbeliard Cedex, France

Geunseop Lee and Hanchul Kim
Division of Chemical Metrology and Materials Evaluation, Korea Research Institute of Standards and Science, P.O. Box 102, Yuseong, Daejeon 305-600, Korea

Jean-Marc Themlin
Groupe de Physique des Etats Condenses, UMR CNRS 6631 Faculte des Sciences de Luminy, 163 Av. de Luminy, Case 901, 13288 Marseille Cedex 9, France
(Received 18 December 2002; published 30 May 2003)

The initial formation of the samarium/silicon interface is studied by combining scanning tunneling microscopy (STM), low-energy electron diffraction, and *ab initio* pseudopotential calculations. A Si(111)3×2-Sm reconstruction is formed at a Sm coverage of 1/6 monolayer. High-resolution STM images reveal a strong bias-voltage dependence for the 3×2 reconstruction. In the empty-state STM images, the rows with a ×2 periodicity are shown at high bias voltages, and attributed to Sm atoms. At low bias voltage, an additional double row feature with a ×1 periodicity appears and dominates the empty-state image as the bias voltage decreases. The paired protrusions with the ×1 periodicity in the double rows in the empty-state image are attributed to Si atoms. In the filled-state STM images, double rows of protrusions forming zigzag chains with a 3×1 structure are observed and assigned to Si atoms. We propose a honeycomb chain-channel model for the 3×2 phase, common to alkali metals and alkaline-earth metals on Si(111). Simulated STM images based on this model are in excellent agreement with experiment.

DOI: 10.1103/PhysRevB.67.195413 PACS number(s): 68.35.−p, 68.37.Ef, 68.43.Bc, 68.55.Jk

I. INTRODUCTION

The adsorption of alkali metals (AM's) and alkaline-earth metals (AEM's) deposited on a Si(111) surface is known to induce 3×1 and 3×2 reconstructions, respectively.[1–7] All of these systems seem to exhibit rowlike arrangements of the adsorbates and a common structure of the Si surface reconstruction. They are very similar in regard to the electronic and structural properties.[7–9] Several structural models have been proposed to accommodate their common features. A model, called as the honeycomb chain-channel (HCC) model,[10] is now considered to be the most plausible candidate since it has the lowest energy among the models proposed so far, and can best account for the experimental results.[10,11]

While AM's and AEM's on Si(111) have been extensively studied, rare-earth metals (REM's) on Si(111) have received much less attention. The REM adsorption on semiconductor surfaces are an interesting subject in regard to the geometric and electronic structures. It is known that the valence of samarium and thereby the number of $4f$ electrons are subject to changes depending on the number of coordination to surrounding atoms.[12] The change in valence of samarium in the Sm-adsorbed Si(111) surface is suggested to be related to the onset of the reactive interdiffusion of Sm and Si.[13] It has been shown through photoelectron spectroscopy measurements that the valence state of the Sm atom changes from divalent ($4f^6 6s^2$) to trivalent ($4f^5 5d\ 6s^2$) with increasing coverage. The driving force of the valence change was suggested to be due to the dangling bond elimination.[14] In the initial adsorption of Sm on Si(111), a 3×2 surface phase [Si(111)3×2-Sm or 3×2-Sm for brevity] was formed. The valence of Sm in the 3×2-Sm surface was found to be in divalent state. From the similarity of Si(111)3×2-Sm and Si(111)3×2-Yb in Si $2p$ core-level spectra, it was proposed that the Sm atoms adsorb in bridge positions on the Si(111) surface.[14,15]

In the present paper, the surface structure of the Si(111)3×2-Sm phase is investigated by combining scanning tunneling microscopy (STM), low-energy electron diffraction (LEED), and *ab initio* pseudopotential calculations. Both LEED and STM indicate that the 3×2-Sm phase is formed at a coverage of 1/6 monolayer (ML) (one Sm atom per 3×2 unit cell). Our high-resolution STM images show a strong bias-voltage dependence of the observed structure, revealing different chain features under different polarities. In the filled-state images, Si zigzag chains with a ×1 periodicity are identified. The empty-state images manifest either Sm atoms with a ×2 periodicity at high bias, or chains of paired Si with a ×1 periodicity at low bias. *Ab initio* calculations find that the HCC model best describes this Si(111)3×2-Sm surface.

II. EXPERIMENT

The STM experiments were performed in an ultrahigh vacuum chamber equipped with an Omicron microscope. The Si(111) substrates (n-type, 0.1 Ω cm resistivity) were cleaned by a repeated cycle of heating at 1200 °C and slow cooling down to room temperature. Sm was evaporated from

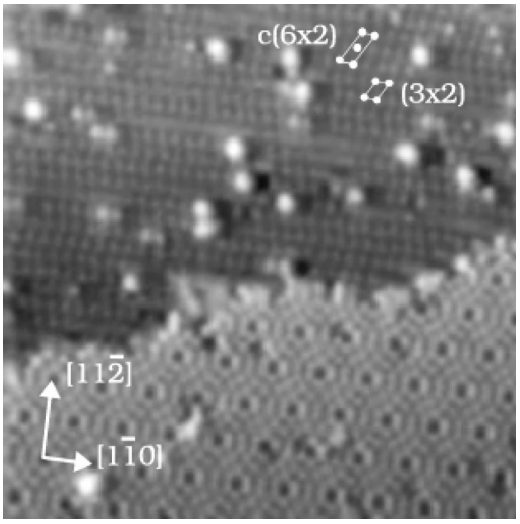

FIG. 1. Empty-state STM image ($V_s=+2$ V) of Sm/Si(111) showing the coexistence of the uncovered Si-7×7 and -3×2 phases. The 3×2 and $c(6\times2)$ unit cells are indicated in the upper part of the image.

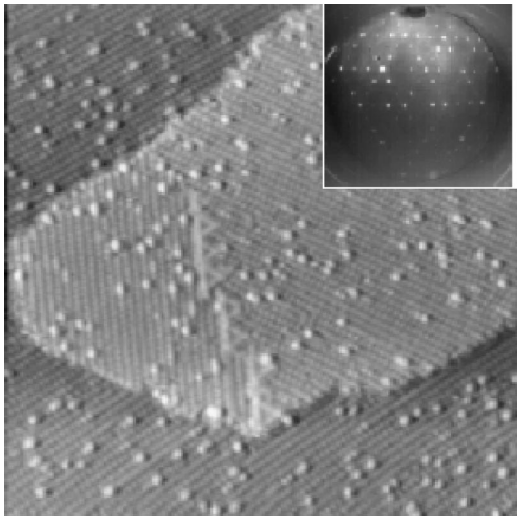

FIG. 2. Large scale STM image showing three domains of the Sm-induced 3×2 phases. The inset is a corresponding LEED pattern showing three domains of 3×1 instead of 3×2.

a Mo crucible and deposited onto the Si(111) substrates at a rate of about 0.63 ML per minute, as monitored by a quartz-crystal oscillator. The ML scale is referred to the Si(111) surface atomic density (7.8×10^{-14} atoms/cm^2). Amounts of 0~1 ML Sm was deposited onto a Si(111)7×7 held at 500 °C and annealed at temperature in the 500–550 °C range. The pressure is better than 3×10^{-10} mbar during the deposition. Both LEED and STM observations were made at room temperature, and the STM images were acquired in the constant current mode.

III. RESULTS AND DISCUSSION

A. The Si(111)3×2-Sm surface

Figure 1 shows a typical empty state STM image taken for a low Sm coverage at a positive sample bias voltage ($V_s=+2$ V). We can observe the coexistence of the Si(111)7×7 (lower part) and the Sm-induced structure (upper part). In the Sm-induced area, parallel rows made of round protrusions run in the $[1\bar{1}0]$ direction. The separation between the rows is $3a$, where $a=(\sqrt{3}/2)a_0=3.32$ Å [$a_0=3.84$ Å, a unit lattice spacing on a bulk terminated Si(111)]. Within the rows, the spacing between the protrusions is $2a_0$. Thus, the Sm-induced reconstructed surface in Fig. 1 has a 3×2 structure.

A close examination of this STM image reveals that the 3×2 order is not perfect. Indeed, along the $[11\bar{2}]$ direction, the 3× periodicity is not preserved due to the occasional out-of-phase shift of protrusions (see the outlined white filled circle, in the upper part of Fig. 1). The structure may be described as a mixture of a 3×2 and a $c(6\times2)$. The 3×2 and the $c(6\times2)$ reconstructions are very similar and are connected by a shift of one unit lattice between two adjacent rows along the $[1\bar{1}0]$ direction. In the following, only the 3×2 reconstruction will be discussed.

The LEED pattern exhibits a 3×1 multidomain structure (inset of Fig. 2). Half-order spots or streaks related to the 3×2 surface reconstruction were not observed. The STM image corresponding to this (3×1) LEED pattern, however, shows the presence of domains of the 3×2 structure rotated by 120° from each other (Fig. 2). The apparent discrepancy between LEED and STM observations on the periodicity of the reconstruction has been already reported for the cases of Ca- and Mg-induced Si(111) reconstructions, incorrectly identified from LEED observations as the 3×1 reconstructions.[3,6,16] This suggests that the structure of the adsorbate atoms in these surfaces does not have long-range order. Taking into account the similarity of the LEED *I-V* curves for 3×1-Li, 3×1-Na, and 3×1-Ag surfaces, it was previously suggested that the LEED reflects the common structure of the top Si layer with the 3×1 reconstruction rather than the structure of the deposited metal atoms.[17] We suppose that the same is applied for 3×2-Sm case where the LEED pattern only reflects the structure of the Si(111) reconstruction while our STM images reveal the structure of both the Si and the adsorbed Sm atoms.

The measurement of the quantity of adsorbed Sm atoms is important to identify the structure. Usually, the quartz-crystal oscillator measurements are not accurate enough to discriminate between 1/3 (*one* Sm atom per 3×2 unit cell) or 1/6 ML (*two* Sm atom per 3×2 unit cell). So we propose, in the following, a way to estimate the Sm coverage with a higher precision. The samarium is evaporated, in ultra high vacuum, on a glass sample at constant rate during several hours. The step height between the initial glass substrate and the samarium layer is then measured by atomic force microscopy. From this measurement, the number of evaporated Sm atoms in ML per minute can be deduced. We obtained 0.63 ML per minute.

Afterward, the Sm is deposited, in the submonolayer range, onto the Si(111)7×7 with the same evaporation rate of 0.63 ML/min. The surface is examined by STM in large scale (not shown), and the fractions of the 7×7 and the

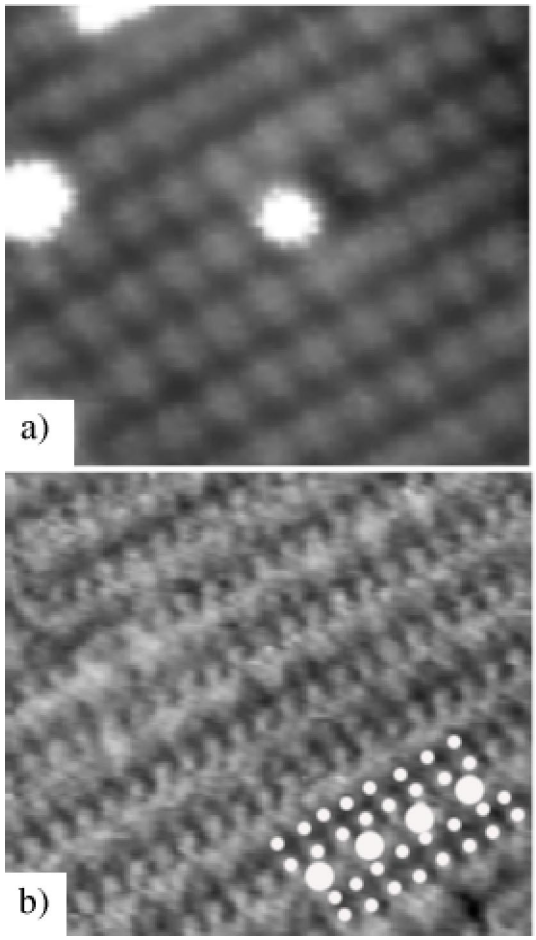

FIG. 3. Atomic resolution STM images of the 3×2 reconstruction acquired at (a) $V_s=+2$ V and (b) $V_s=+1.7$ V.

3×2 phases are determined. A surface fully covered by the 3×2 phase is obtained for a coverage of $1/5\pm1/25$ of ML. Therefore, the Sm coverage appears to be 1/6 ML rather than 1/3 ML for the 3×2 phase. This estimate is compatible with the observation of a single protrusion per 3×2 cell in STM. The 3×2 protrusions are therefore assigned to Sm atoms. These observations for the Si(111)3×2-Sm phase in the empty-state STM images at +2 V bias suggest a close resemblance to the Si(111)-3×2 phases induced by others AEM adsorbates.

B. The STM bias-voltage dependence of the 3×2 reconstruction

The bias-voltage dependence of the STM image of the Si(111)3×2-Sm reconstruction is shown in Fig. 3. Figures 3(a) and 3(b) show atomic-resolution empty-state images taken at sample bias voltages of $V_s=+2$ V and $V_s=+1.7$ V, respectively. There are apparent differences between these STM images. Figure 3(a) is similar to the one presented in Fig. 1, showing rows of protrusions with the intrarow spacing of $2a_0$. Figure 3(b) shows an appearance of an additional feature, double rows of weak protrusions, between the ×2 rows (or bright lines). These secondary protrusions look similar to spurs extending to both sides of the main rows, making the main rows ragged. While the distance between the main protrusions in a bright line is mostly $2a_0$, the spacing between the small spurs along each row is $1a_0$. Note that the position of the 3×2 protrusions in Fig. 3(a) corresponds to the ragged bright lines in Fig. 3(b).

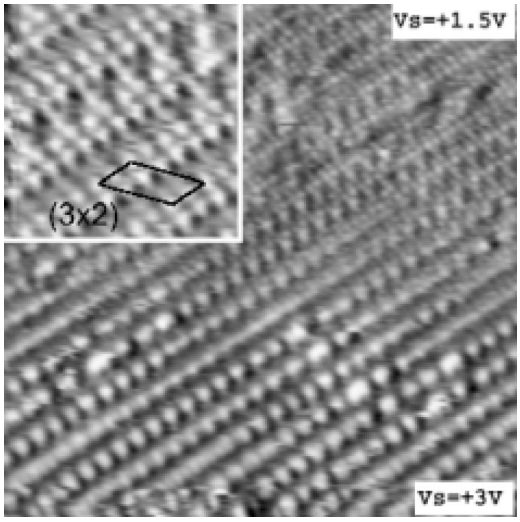

FIG. 4. STM image showing the bias-voltage dependence in the empty state. The bias voltage is increased during the scan from $V_s=+1.5$ V (top of the image) to $V_s=+3$ V (bottom of the image). A zoomed-in image of the upper part is shown in the inset.

Figure 4 shows an empty-state image where the sample bias voltage is changed during the scan, revealing the bias-voltage dependence. The large, well-defined protrusions, observed in Fig. 3(a) and assigned to the Sm atoms, are clearly visible at the bottom of the image scanned with $V_s=+3$ V. When the bias voltage is decreased, the atomic resolution of these protrusions becomes poor and forms the periodic corrugation observed in Fig. 3(b). At lower bias voltage of $V_s=+1.5$ V, the changes from the image with $V_s=+3$ V are much more distinguishable. The image becomes dominated by double rows consisting of paired protrusions with $1a_0$ spacing in the row direction. A close inspection reveals that the paired protrusions correspond to the side spurs observed in the intermediate bias voltage [see Fig. 3(b)]. The ×2 protrusions which appear as the exclusive or dominant features in the image with higher bias voltage become weaker with decreasing bias voltage. These characteristics of the low-bias, empty-state image are clearly visible in the inset of Fig. 4.

The filled-state image of 3×2-Sm was obtained with atomic resolution, as shown in Fig. 5. There are bright double rows running in the $[1\bar{1}0]$ direction separated by dark channels. The protrusions in the double rows form zigzag chains with the ×1 periodicity. Thus, the apparent unit cell formed by these protrusions is a 3×1. The zigzag chain feature in the filled-state image is nearly identical to those reported for the Si(111)3×2-Ba phase as well as for the Si(111)3×1-AM surfaces.[5]

The double rows observed in the filled-state image differ from those observed in the empty-state image at low positive bias voltage (upper part of Fig. 5): the former constituting

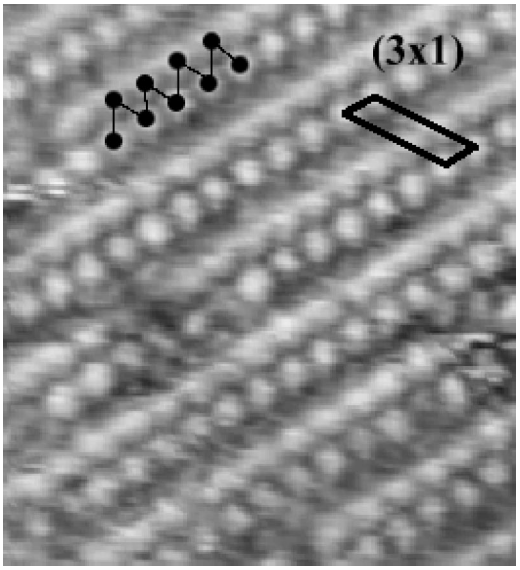

FIG. 5. A high-resolution filled-state STM image acquired at $V_s = -1.5$ V. The zigzag chains form a 3×1 structure rather than a 3×2 structure.

zigzag chains and the latter being paired double rows. Both double-row features are attributable to Si atoms, because only the 3×2 protrusions in the empty-state STM images at high bias voltage can be naturally assigned to Sm atoms based on the coverage of 1/6 ML. The polarity dependence of those double-row features indicates different electronic characters of the two types of Si atoms observed in the filled- and the empty-state STM images. The relative registry between the surface Si atoms as well as the Sm atoms can be deduced if both filled- and empty-state images are taken simultaneously in dual-bias scan. Unfortunately, we could not obtain the dual-bias images with a good resolution, and have no information on the registration of the Si and Sm atoms on the surface. However, those Si features seen in the STM images unambiguously indicate the reconstruction of the Si substrate. This invalidates the previously proposed model[14] where Sm atoms adsorb in bridge positions on the bulk-terminated Si(111)1×1 surface.

C. Honeycomb chain-channel (HCC) model and simulated STM images

Our experimental results provide insight into the structure of the Si(111)3×2-Sm phase. While the Sm atoms arrange in a 3×2 structure, the apparent structure of the Si atom arrangement is 3×1. The 3×1 structure is common to the reconstruction of the Si(111) surface induced by different AM's and AEM's. A number of structural models have been proposed to describe this reconstruction. A few years ago, the HCC model, named by Erwin *et al.*, was found to be the energetically most favorable.[10] Consistent with the results obtained by different analysis techniques, the HCC model seems to be accepted by the community. Recently, the Si(111)3×2-Ba surface has also been described in terms of the HCC model.[5] It was claimed that the Si(111)3×2-Ba surface consists of the HCC-reconstructed Si substrate and Ba atoms of 1/6 ML coverage. The period doubling observed in the filled-state Si feature was viewed as a structural perturbation due to the Ba occupancy in every other 3×1 cell.

Taking into account the information provided by the coverage, the registration, and the polarity dependence of the STM images, we believe that the double rows of protrusions seen in filled- and empty-state STM images represent two types of Si surface atoms with different electronic characters. They reflect the Si substrate reconstruction. These experimental results suggest a close resemblance between the Si(111)3×2-Sm surface structure and that of the Si(111)3×2-Ba. Our observations are in obvious contradiction with previously reported model in which the Sm atoms adsorb in bridge positions on the Si(111)1×1 surface.

Taking into account the information provided by the coverage measurement and the STM images, we also propose that Si(111)3×2-Sm reconstruction can be described by the HCC model. The substrate structure is basically a 3×1 reconstruction formed by four inequivalent Si adatoms which form a ''honeycomb chain'' parallel to the plane surface. These four Si atoms are threefold coordinated and the inner atoms are in a planar configuration. The 1/6 ML of the adsorbed Sm atoms occupy every other 3×1 cell. This renders the substrate structure being subject to modification to the 3×2 periodicity.

To validate the HCC model with 1/6 ML Sm for the Si(111)3×2-Sm surface, we have performed *ab initio* calculations within the generalized gradient approximation (GGA) (Ref. 18) using the Vienna *ab initio* simulation package (VASP).[19,20] The 3×2 surface is modeled by a slab which is composed of a Sm atom, eight Si atoms forming HCC, four Si layers, and a H layer passivating the bottom surface. The Sm atom is represented by projector-augmented-wave (PAW) potential[21,22] and the Si and H atoms are represented by ultrasoft pseudopotentials as provided with VASP.[23,24] We used a kinetic energy cutoff of 180 eV and 4×6 k-point mesh within the surface Brillouin zone. With the use of the self-consistent Kohn-Sham eigenvalues and wave functions, the constant-current STM images are simulated within the Tersoff-Hamann scheme.[25,26]

The 1/6 ML Sm coverage was accommodated by putting one Sm atom in every second 3×1 unit cell of the HCC structure. Two different adsorption sites T_4 and H_3 in the channel were considered (see Fig. 6). The surface energies for T_4 and H_3 sites are comparable; the former being lower by only 0.07 eV/Sm. The equilibrium geometry for the T_4 site is shown in Fig. 6. The presence of Sm atoms in the channel induces a structural modification of the 3×1 HCC structure. Most prominently, the honeycombs are deformed. The deformations of the neighboring honeycombs, however, are not equivalent: One honeycomb is more elongated in $[11\bar{2}]$ direction, perpendicular to the chain, than the adjacent ones. The other noticeable deformation occurs at the left edge of the honeycomb chain (denoted as l in Fig. 6): Along the chain, the corrugations are 0.08 Å in height and 0.18 Å in the lateral displacement perpendicular to the chain, respectively. In the right edge (denoted as r in Fig. 6), the deformation is hardly recognizable. Consequently, the substrate

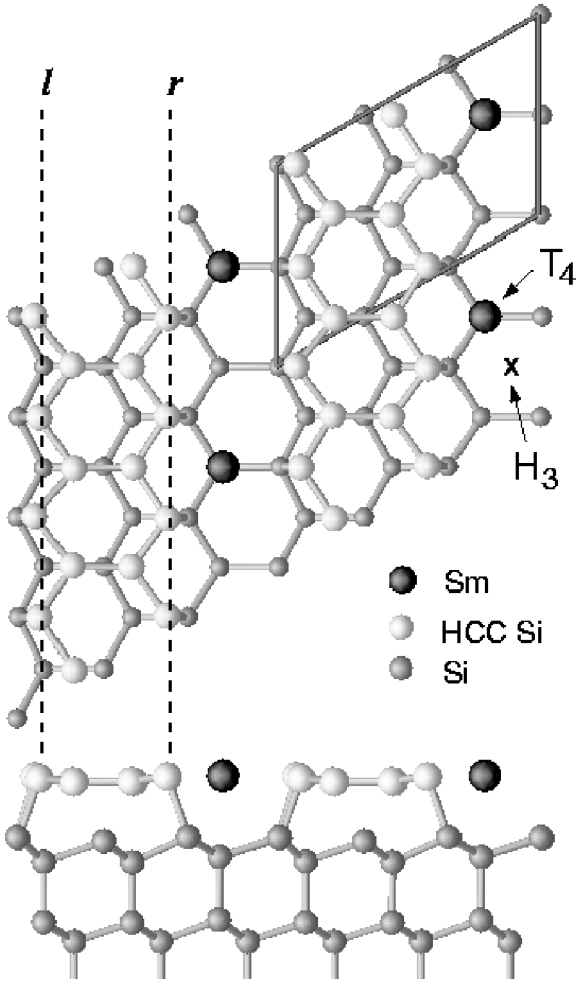

FIG. 6. Honeycomb chain-channel (HCC) model for the Si(111)3×2-Sm surface.

reconstruction, as well as the Sm adsorption, adopts ×2 periodicity along the chain direction. Two inner Si atoms of each honeycomb form a double bond, as in the cases of 3×1-AM and 3×2-Ba. The double-bond length is 2.28 Å.

It is worthwhile to compare the structural characteristics of the 3×2-Sm surface to that of the 3×2-Ba surface. The aforementioned structural change along *l* in Fig. 6 is smaller in magnitude compared to the case of Ba: The corrugations for Ba/Si(111) are 0.13 Å in height and 0.4 Å in the lateral displacement. In addition to the substrate structural modification, the Sm atom is located 0.23 Å higher than the inner Si atoms of the honeycomb chain. In contrast, the Ba atom is located 0.75 Å higher than the inner Si atoms. From these differences, we can expect that the degree of period doubling in the filled-state STM image should be weaker for 3×2-Sm than for 3×2-Ba. Also in the empty-state STM images, the Si=Si double bond might be visible in conjunction with the Sm ions for 3×2-Sm.

The STM simulation well reproduces the experimental images both for the filled states and for the empty states. In the filled-state image shown in Fig. 7(a), the double row of bright protrusions are formed. The protrusions form zigzag chain structure connecting two neighboring honeycombs across a channel. This filled-state feature is the manifestation of the saturated dangling-bond states of the Si atoms surrounding Sm. A closer look at the filled-state STM image unveils a weak pairing of Si atoms in the *r* row (see Fig. 6), similarly to the case of Ba-induced 3×2 surface. The pairing is caused by the electrostatic attraction between a positively ionized Sm atom and the electrons in two neighboring saturated dangling bonds on the *r*-row Si atoms. The dangling bond electrons are pulled towards the neighboring Sm atom. Similarly, a Sm atom attracts the dangling bond electrons of the nearest Si atom in the *l* row (see Fig. 6). This compensates the corrugation in lateral displacement (where the Si atom is relaxed away from the Sm chain) and results in almost aligned bright spots in the *l* row. Interestingly, the pairing of Si atoms along the $[1\bar{1}0]$ direction is barely observed in our experimental images, in contrast to the 3×2-Ca and the 3×2-Ba surfaces for which the pairing was experimentally observed.[1,5] This may be attributed to the fact that the structural modification due to the metal atoms is smaller in magnitude for 3×2-Sm compared with 3×2-Ba.

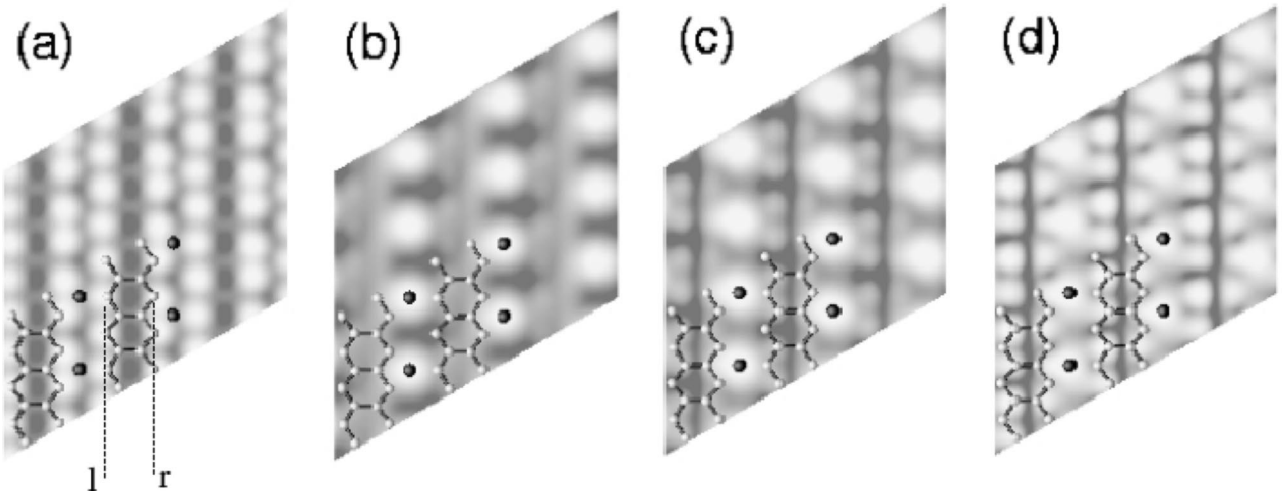

FIG. 7. Simulated STM images of Si(111)3×2-Sm: (a) a filled-state image at $V_s=-2.0$ V and (b)–(d) empty-state images at $V_s=+2.0$, $+1.5$, and $+1.0$ V, respectively.

Compared to the filled-state images, the empty-state images, shown in Figs. 7(b)–7(d), reveal strong bias dependence. At high biases ($>+2.0$ V), the Sm atoms are manifested as rows of bright protrusions with $\times 2$ periodicity. For the lower bias voltages [Figs. 7(c) and 7(d)], a feature appears in the form of additional double rows of protrusions with $\times 1$ period. This additional feature is located at the inner Si atoms that form the Si=Si double bond, and is attributed to the empty $\pi^{\star}$ antibonding orbitals of the double bond. The manifestation of the Si double bond as a main feature at low biases is due to the fact that the Sm atoms take adsorption sites closer to the substrate if compared with the Ba atoms as described above.

IV. SUMMARY AND CONCLUSION

The surface structure of the Si(111)3×2-Sm phase obtained for a 1/6 ML Sm coverage is investigated by combining STM, LEED, and *ab initio* calculations. While the LEED exhibits a (3×1) pattern, the STM images reveal the 3×2 structure. The apparent discrepancy between LEED and STM observations is explainable by the lack of the LEED sensitivity to the Sm atoms in poor long-range order. The 3×1 LEED pattern reflects the well-ordered reconstruction structure of the top Si layer.

High resolution STM images show a strong bias-voltage dependence of the observed structure, revealing different chain features for opposite polarities. In the filled states, zigzag chains with a 3×1 periodicity are observed and assigned to the saturated dangling bond states of the Si atoms in the reconstruction. In the empty states, we observe both rows of protrusions with a 3×2 periodicity and double rows consisting of paired protrusions with a 3×1 periodicity, depending on the magnitude of the bias voltage. They are attributed to the Sm atoms and the empty $\pi^{\star}_{\text{Si-Si}}$ antibonding orbitals, respectively. The empty-state images vary from the Sm feature (3×2 registry) for the high bias voltage to the Si feature (3×1 registry) for the low bias voltage.

These STM observations are incompatible with the previous model proposed for this system, in which the Sm atoms adsorb in bridge positions on the Si(111)1×1 surface. Instead, they are in good agreement with the HCC model proposed for the Si(111)3×2-Ba surface, as verified by the theoretical calculations. We propose that the Si(111)3×2-Sm surface consists of the HCC-based Si substrate reconstruction structure and Sm adsorbate atoms with 1/6 ML coverage. We further contend that the prerequisite of one donated electron per 3×1 unit cell resulting in the common Si(111)3×1 substrate reconstruction is also applied to the cases of the divalent REM adsorbates such as Sm and Yb.

ACKNOWLEDGMENTS

G.L. appreciates support by KOSEF through ASSRC. H.K. acknowledges the use of the computing facilities of the Supercomputing Center at the Korea Institute of Science and Technology Information through ''The Fifth Strategic Supercomputing Support Program''. Both G.L. and H.K. are also grateful for partial support by MOST through the National Science and Technology Programs (Grant No. M1-0221-00-0007).

*Electronic address: frank.palmino@pu-pm.univ-fcomte.fr

[1] A. Baski, S. Erwin, M. Turner, K. Jones, J. Dickinson, and J. Carisle, Surf. Sci. **476**, 22 (2001).
[2] J. Pagel, G. Neuhold, H. Haak, and K. Horn, Surf. Sci. **414**, 221 (1998).
[3] O. Kubo, A. Saranin, A. Zotov, V. Lifshits, M. Katayama, K. Oura, T. Harada, H. Tani, and J.-T. Ryu, Surf. Sci. **415**, L971 (1998).
[4] A. Saranin, A. Zotov, V. Lifshits, M. Katayama, and K. Oura, Surf. Sci. **426**, 298 (1999).
[5] G. Lee, S. S. F. Hong, H. Kim, D. Shin, J. Koo, H. Lee, and D. Moon, Phys. Rev. Lett. **87**, 56 104 (2001).
[6] D. Jeon, T. Hashizume, and T. Sakurai, J. Vac. Sci. Technol. B **12**, 2044 (1994).
[7] K. Wan, X. Lin, and J. Nogami, Phys. Rev. B **46**, 13 635 (1992).
[8] H. Weitering, N. DiNardo, R. Perez-Sandoz, J. Chen, and E. Mele, Phys. Rev. B **49**, 16 837 (1994).
[9] C. Jeon, T. Hashizume, T. Sakurai, and R. Willis, Phys. Rev. Lett. **69**, 1419 (1992).
[10] S. Erwin and H. Weitering, Phys. Rev. B **81**, 2296 (1998).
[11] M. Kang, J. Kang, and S. Jeong, Phys. Rev. B **58**, 13 359 (1998).
[12] A. Stenborg, O. Bäjrneholm, A. Nilsson, N. Märtensson, J. Andersen, and C. Wigren, Phys. Rev. B **40**, 5916 (1989).
[13] A. Franciosi, J. Weaver, P. Perfetti, A. Katnani, and G. Margaritondo, Solid State Commun. **47**, 427 (1983).
[14] C. Wigren, J. Andersen, R. Nyholm, M. Goyhelid, M. Hammar, C. Tornevik, and U. Karlson, Phys. Rev. B **48**, 11 014 (1993).
[15] C. Wigren, J. Andersen, R. Nyholm, U. Karlson, J. Nogami, A. Baski, and C. Quate, Phys. Rev. B **47**, 109 (1993).
[16] T. Urano, K. Wanatanabe, and S. Hongo, Surf. Sci. **169/170**, 88 (2001).
[17] W. Fan and A. Ignatiev, Phys. Rev. B **41**, 3592 (1990).
[18] J. P. Perdew, J. A. Chevary, S. H. Vosko, K. A. Jackson, M. R. Pederson, D. J. Singh, and C. Fiolhais, Phys. Rev. B **46**, 6671 (1992).
[19] G. Kresse and J. Hafner, Phys. Rev. B **47**, 558 (1993).
[20] G. Kresse and J. Furthmuller, Phys. Rev. B **54**, 11 169 (1996).
[21] P. Blochl, Phys. Rev. B **50**, 17 953 (1994).
[22] G. Kresse and J. Joubert, Phys. Rev. B **59**, 1758 (1999).
[23] D. Vanderbilt, Phys. Rev. B **41**, 7892 (1990).
[24] G. Kresse and J. Hafner, J. Phys.: Condens. Matter **6**, 8245 (1994).
[25] J. Tersoff and D. R. Hamann, Phys. Rev. Lett. **50**, 1998 (1983).
[26] J. Tersoff and D. Hamann, Phys. Rev. B **31**, 805 (1985).